

## ORIGINAL ARTICLE

## An antibody to amphiregulin, an abundant growth factor in patients' fluids, inhibits ovarian tumors

S Carvalho<sup>1,10</sup>, M Lindzen<sup>1,10</sup>, M Lauriola<sup>1,9</sup>, N Shirazi<sup>1</sup>, S Sinha<sup>1</sup>, A Abdul-Hai<sup>2</sup>, K Levanon<sup>3</sup>, J Korach<sup>4</sup>, I Barshack<sup>5</sup>, Y Cohen<sup>6</sup>, A Onn<sup>7</sup>, G Mills<sup>8</sup> and Y Yarden<sup>1</sup>

Growth factors of the epidermal growth factor (EGF)/neuregulin family are involved in tumor progression and, accordingly, antibodies that intercept a cognate receptor, epidermal growth factor receptor (EGFR)/ERBB1, or a co-receptor, HER2, have been approved for cancer therapy. Although they might improve safety and delay onset of chemoresistance, no anti-ligand antibodies have been clinically approved. To identify suitable ligands, we surveyed fluids from ovarian and lung cancer patients and found that amphiregulin (AREG) is the most abundant and generalized ligand secreted by advanced tumors. AREG is a low affinity EGFR ligand, which is upregulated following treatment with chemotherapeutic drugs. Because AREG depletion retarded growth of xenografted ovarian tumors in mice, we generated a neutralizing monoclonal anti-AREG antibody. The antibody inhibited growth of ovarian cancer xenografts and strongly enhanced chemotherapy efficacy. Taken together, these results raise the possibility that AREG and other low- or high-affinity binders of EGFR might serve as potential targets for cancer therapy.

*Oncogene* (2016) 35, 438–447; doi:10.1038/onc.2015.93; published online 27 April 2015

## INTRODUCTION

Growth factors and their cognate receptors are involved in all steps of tumor progression, especially in the evasion from the toxic effects of chemo- and radiotherapy.<sup>1–3</sup> An example is provided by the epidermal growth factor (EGF) receptor (EGFR) family of tyrosine kinases, and their EGF-like ligands. The family comprises four receptors (EGFR/ERBB1/HER1, ERBB2/HER2, ERBB3/HER3 and ERBB4/HER4) and eleven ligands, polypeptides of the EGF/neuregulin (NRG) family. These ligands can be classified according to their affinity to EGFR: while none of the NRGs binds with EGFR, EGF, transforming growth factor alpha (TGF- $\alpha$ ), heparin-binding EGF (HB-EGF) and betacellulin (BTC) are considered as high-affinity ligands.<sup>4</sup> By contrast, amphiregulin (AREG), epi-regulin (EREG) and epigen (EPG) are considered as low-affinity ligands.<sup>5</sup> Following binding of high-affinity ligands, EGFR is rapidly internalized from the cell surface, which results in signal attenuation. Although high-affinity ligands stimulate a strong and robust response, the burst of activation is short lived due to potent negative feedback loops.<sup>6,7</sup> Interestingly, under certain conditions the low-affinity ligands, including an engineered ligand, display relatively high mitogenic potency due to incompletely understood mechanisms.<sup>5,8–10</sup> This phenomenon is also observed with the many EGFR ligands encoded by poxviruses. These viral ligands display lower receptor binding affinity, as compared with their mammalian counterparts, but their biological activities are sometimes more potent.<sup>9</sup>

Of the low-affinity ligands, AREG is increasingly recognized for the key roles it plays in both normal and disease contexts. Human AREG is located on chromosome band 4q14.3; AREG is flanked on

the 5' region by its family members *EREG* and *EPG*, and on the 3' region by another kin, *BTC*. The gene is composed of six exons that encode a 1.4-kb mRNA (reviewed in Berasain and Avila<sup>11</sup>). The corresponding protein is synthesized as a 252 amino-acid transmembrane precursor (pro-AREG), which undergoes proteolytic cleavage within its ectodomain, thereby releasing a biologically active soluble protein. This process is mediated by the tumor-necrosis factor- $\alpha$  converting enzyme (TACE, also known as ADAM 17). EGFR can be activated by AREG through several mechanisms: autocrine or paracrine activation by the soluble form of AREG, a juxtacrine mode enabling the un-cleaved transmembrane form to activate EGFR,<sup>12</sup> or by a newly described mode entailing AREG containing exosomes.<sup>13</sup> AREG has pivotal roles in mammary gland development,<sup>14</sup> as well as in branching and morphogenesis occurring within several epithelial tissues. Conversely, AREG has also been extensively linked to the oncogenic process. AREG expression has been associated with worse prognosis of several cancers, including prostate, pancreatic, breast, lung, and head and neck tumors.<sup>11</sup>

The present study addresses the therapeutic potential of intercepting AREG. First, we profiled the repertoire of EGF-family ligands in fluids obtained from ovarian and lung cancer patients. The results identified AREG as one of the most abundant EGF-like growth factors secreted by advanced forms of both tumor types. We also confirmed in ovarian cancer cells that AREG evades EGFR's negative feedback regulation, as well as demonstrated a stimulatory effect of chemotherapy on AREG secretion. In line with these observations, we found that knocking-down AREG expression in human ovarian cancer cells delayed the onset of

<sup>1</sup>Department of Biological Regulation, Weizmann Institute of Science, Rehovot, Israel; <sup>2</sup>Kaplan Medical Center, Rehovot, Israel; <sup>3</sup>The Dr. Pinchas Borenstein Talpiot Medical Leadership Program and Institute of Oncology, The Institute of Oncology, Chaim Sheba Medical Center, Ramat Gan, Israel; <sup>4</sup>Department of Gynecologic Oncology, Chaim Sheba Medical Center, Ramat Gan, Israel; <sup>5</sup>Department of Pathology, Sheba Medical Center, Ramat Gan, Israel; <sup>6</sup>Institutional Tissue Banks, Sheba Medical Center, Ramat Gan, Israel; <sup>7</sup>Institute of Pulmonary Oncology, Chaim Sheba Medical Center Ramat Gan, Israel and <sup>8</sup>Department of Systems Biology, The University of Texas MD Anderson Cancer Center, Houston, TX, USA. Correspondence: Dr Y Yarden, Department of Biological Regulation, The Weizmann Institute of Science, 76100 Rehovot, Israel. E-mail: yosef.yarden@weizmann.ac.il

<sup>9</sup>Current address: Unit of Histology, Embryology and Applied Biology, Department of Experimental, Diagnostic and Specialty Medicine, University of Bologna, Bologna 40126, Italy.

<sup>10</sup>These authors contributed equally to this work.

Received 12 October 2014; revised 26 February 2015; accepted 27 February 2015; published online 27 April 2015

tumor xenografts. Ultimately, we raised a neutralizing anti-AREG monoclonal antibody (mAb) that effectively inhibited ovarian cancer xenografts, especially when combined with a genotoxic drug commonly used to treat ovarian cancer patients. Altogether, our results support the contention that targeting AREG with neutralizing antibodies might represent an effective anti-cancer strategy.

## RESULTS

High abundance of AREG in fluids from cancer patients, as well as in media conditioned by cancer cells

Due to the established roles for a variety of growth factors in cancer progression (reviewed in Witsch *et al.*<sup>1</sup>), we used enzyme-linked immunosorbent assay (ELISA) to determine the repertoire of EGF-like ligands present in fluids collected from advanced stage ovarian and lung cancer patients. Ascites collected from 43 ovarian cancer patients, who were previously treated with chemotherapy, identified AREG as one of the two most frequently secreted factors (Figure 1a, Supplementary Figure S1a and Supplementary Table 1): 37 out of the 43 patients (86%) expressed AREG, with levels displaying wide variation (10–1800 pg/ml). The ELISA analysis similarly identified TGF- $\alpha$  in 88% of the analyzed patients, but HB-EGF (60%), EGF (44%), NRG1 (21%) and BTC (6.9%) were not only detected in fewer patients, but their levels rarely exceeded 200 pg/ml. A related pattern was observed in media conditioned by 13 ovarian cancer cell lines (Figure 1c): AREG (92% of the analyzed cell lines), TGF- $\alpha$  (69%), HB-EGF (54%) and NRG1 were detectable, though the latter was observed in only one cell line. Notably, EGF was undetectable in the conditioned media, but we were able to detect EGF, albeit at low levels, in 44% of patients' fluids, raising the possibility of a

non-tumor origin. Similarly, we were unable to detect BTC in any ovarian cancer cell line, but a minority of patients' ascites fluids contained this growth factor. Note that due to the unavailability of ELISA kits, we could not assay other EGF-family ligands.

A parallel analysis was performed on pleural effusions from lung cancer patients (Figure 1b, Supplementary Figure S1b and Supplementary Table 2). Similar to the ovarian ascites fluids, the major growth factor detected in pleural effusions from lung cancer patients was AREG: 16 of 18 samples contained relatively high concentrations of the factor. Also similar to ovarian cancer, approximately 50% of the lung cancer pleural fluids contained TGF- $\alpha$  and HB-EGF. Analysis of the conditioned media of seven lung cancer cell lines identified AREG as a common and almost exclusive trait (Figure 1d); no other ligand, with the exception of HB-EGF (in H522 cells), was detectable. Taken together, these results identify AREG as a most prevalent EGF-like growth factor of both ovarian and lung cancers.

AREG is less efficient at receptor downregulation and degradation than EGF or TGF- $\alpha$

The observed wide distribution and high concentrations of AREG in patients' fluids raised the possibility that this factor confers a selective advantage, which may not be shared by other EGF-like ligands.<sup>11</sup> Hence, we compared the biological activities of AREG with those of the better-understood family members. It is notable that George Todaro and colleagues,<sup>15</sup> who discovered AREG in 1989, reported that it binds to EGFR but not as avidly as EGF; nevertheless, it fully supplants the requirement for EGF or TGF- $\alpha$  in keratinocyte growth.<sup>15</sup> These early observations might relate to the duration of inducible EGFR signaling, which is directly correlated to binding affinity and the intracellular fate of ligand-bound EGFR:<sup>16,17</sup> depending on ligand identity, occupied EGFRs

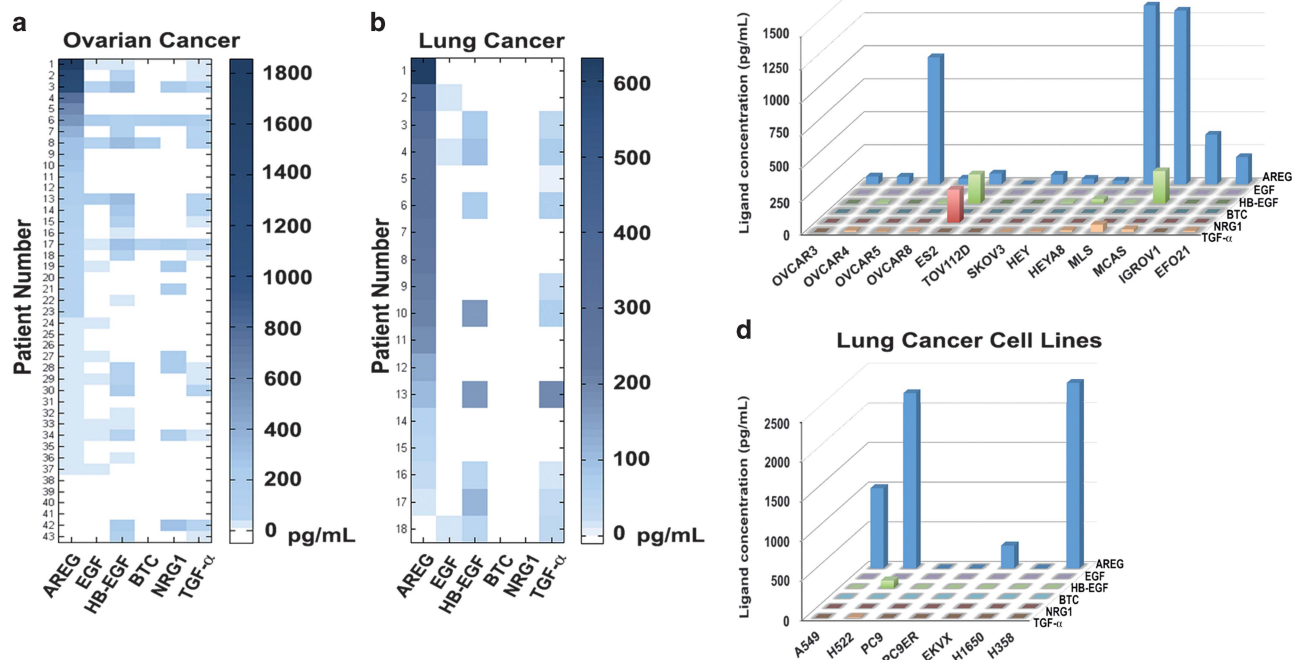


**Figure 1.** High abundance of AREG in fluids from ovarian and lung cancer patients and in media conditioned by ovarian cancer cells. **(a)** Heatmap representation of the abundance of the indicated EGF-family ligands as determined using ELISA and 43 ascites fluids collected from patients with ovarian cancer. The color range is depicted (right column). **(b)** Pleural effusion fluids collected from 18 lung cancer patients were analyzed as in **(a)**. **(c)** The indicated 13 ovarian cell lines were seeded in 10-cm plates, covered with medium (6 ml), and incubated for 4 days. Media were collected and the specified ligands were quantified using ELISA. **(d)** A panel of seven lung cancer cell lines was analyzed as in **(c)**.

will either undergo degradation or recycle back to the plasma membrane, establishing a pool of unliganded receptor for re-activation. To specifically address relationships between binding affinity and receptor endocytosis, we used the mucinous cystadenocarcinoma (MCAS) ovarian cancer cell line. As expected, displacement of a radiolabeled EGF by AREG supported an approximately 100-fold lower binding affinity compared with EGF (Figure 2a). This difference was observed also in MCF10A immortalized mammary cells (Supplementary Figure S2a), suggesting independence from cellular context. In line with relatively low affinity, we observed only limited effect of AREG on endocytosis-mediated downregulation of EGFR (Figure 2b); while EGF (10 ng/ml) induced approximately 80% downregulation following 30–40 min of incubation, and TGF- $\alpha$  (10 ng/ml) achieved 70–75% reduction, AREG (50 ng/ml) induced only approximately 30% receptor downregulation. Similarly, using MCF10A cells and either equimolar concentrations of EGF, TGF- $\alpha$  and AREG, or a 100-fold higher concentration of the latter ligand (Supplementary Figure S2b), we observed effective downregulation of EGFR only with very high concentrations of AREG. These observations are in line with the lower apparent affinity of AREG, as compared with EGF and TGF- $\alpha$ , and they propose that the observed, relatively high concentrations of AREG in patients' fluids are due, in part, to inefficient removal of this ligand by means of receptor-mediated endocytosis and subsequent degradation.

AREG induces relatively weak ubiquitination of EGFR

Early observations demonstrated that EGFR signals undergo rapid desensitization through endocytosis, followed by degradation in lysosomes, and later studies associated this process with receptor ubiquitination.<sup>18</sup> We, therefore, compared the capabilities of EGF, TGF- $\alpha$  and AREG to induce ubiquitination of EGFR in human ovarian cancer cells (MCAS and MLS), as well as in lung cancer cells (H358 and A549; Figure 2c). To this end, cells were incubated for 10 min with the respective growth factor, and subsequently EGFR ubiquitination was detected by western blotting. Whereas EGF and TGF- $\alpha$  induced strong ubiquitination and initiated receptor degradation, similar concentrations of AREG failed to do so, in line with previous reports that used other cell types.<sup>19–21</sup> Interestingly, a 10-fold higher concentration of AREG was capable of inducing high levels of receptor ubiquitination, similar to EGF and TGF- $\alpha$ , suggesting that the lower binding affinity of AREG was responsible for this effect. Notably, the same phenomenon was observed in both the ovarian and the lung cancer cell lines, attesting to a general mechanism, which is cell type independent. Note, however, that receptor ubiquitination and degradation were more closely associated in the lower expressors lung cancer cells, in line with overexpression-induced retardation of EGFR degradation (reviewed in Zwang and Yarden<sup>22</sup>). In conclusion, unlike high-affinity EGFR ligands, AREG fails to induce receptor endocytosis and ubiquitination, and thus signaling desensitization is

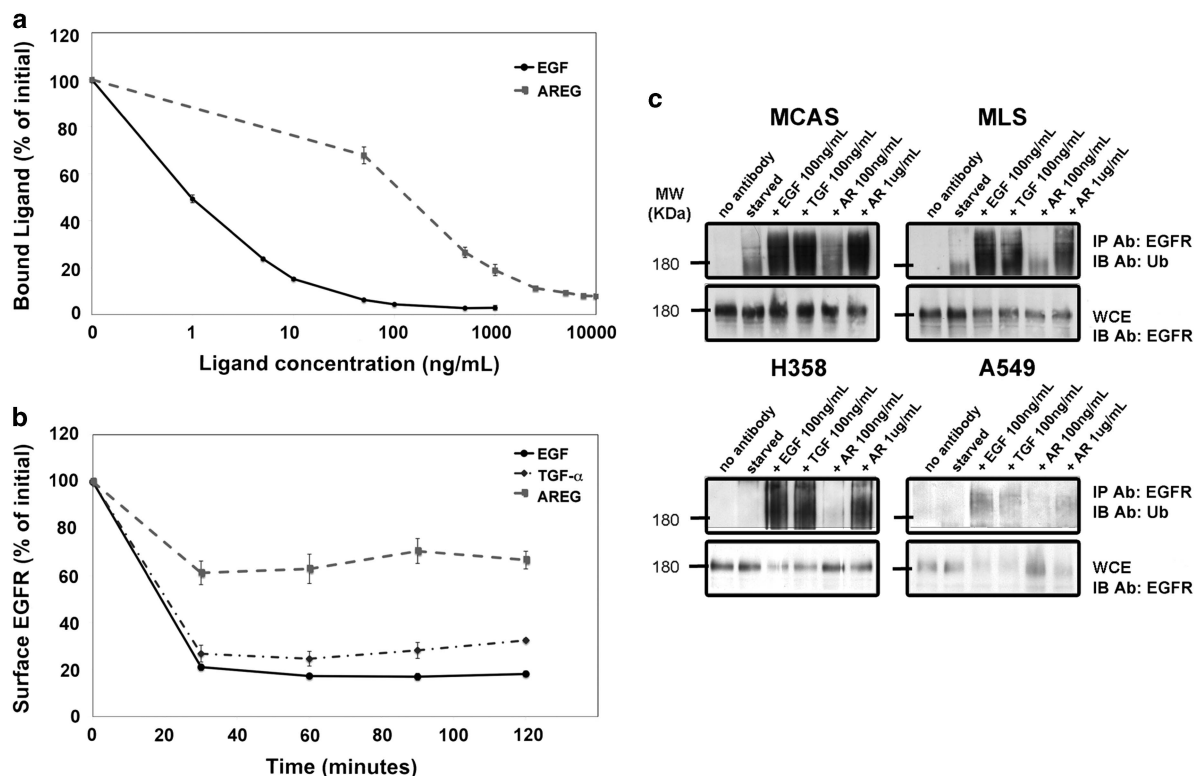


**Figure 2.** AREG is a low-affinity ligand that induces limited receptor downregulation, as well as weak ubiquitination and degradation of EGFR. (a) MCAS ovarian cancer cells were plated in 12-well plates and incubated for 3 h on ice with a radiolabeled EGF ( $^{125}$ I-EGF; 50 ng/ml) in the absence or presence of increasing concentrations of the indicated competing (unlabeled) ligand. The cells were later washed and lysed, and associated radioactivity was determined. The extent of ligand displacement (mean  $\pm$  range of triplicates) was plotted with respect to binding in the absence of an unlabeled ligand. (b) MCAS ovarian cells were incubated in a 12-well plate and starved overnight for serum factors. On the following day, cells were stimulated (or un-stimulated) with EGF (10 ng/ml), TGF- $\alpha$  (10 ng/ml) or AREG (50 ng/ml) for 30, 60, 90 and 120 min. Next, cells were transferred to 4 °C and EGFR downregulation was assayed following exposure to a radioactive EGF ( $^{125}$ I-EGF; 50 ng/ml) for 60 min. The cells were later washed and lysed in 1N NaOH. Cell-associated radioactivity was determined. Averages of triplicates and s.d. values (bars) are presented. (c) Whole extracts of the ovarian cancer cell lines MCAS and MLS, as well as the lung cancer cell lines H358 and A549, that were pre-stimulated for 10 min with EGF (100 ng/ml), TGF- $\alpha$  (100 ng/ml) or AREG (100 ng/ml or 1  $\mu$ g/ml) were subjected to immunoprecipitation (IP) of EGFR. Washed immunocomplexes, along with whole extracts, were immunoblotted with the indicated antibodies.



weakened, potentially explaining why advanced ovarian and lung tumors frequently secrete this factor.

Induction of gene expression programs requires relatively high concentrations of AREG

EGFR activation and the cytoplasmic signaling events it evokes translate to the induction of complex gene expression programs, which, among other functions, propel positive and negative feedback regulatory loops. Because previous reports have not determined the concentration dependence of AREG-induced gene expression programs, we applied high and low concentrations (10 and 100 ng/ml) and used qPCR to analyze several components of both positive (that is, the early induced ligands of EGFR, namely EREG, TGF- $\alpha$  and HB-EGF) and negative feedback regulatory loops. The latter comprised MIG6/RALT, an inducible inhibitor of EGFR,<sup>23</sup> along with two members of the DUSP/MKP dual specificity phosphatase family.<sup>24</sup> In line with low affinity and weak activity, the lower concentration of AREG induced hardly detectable signals, but the 10-fold higher concentration resulted in a clear, time-dependent increase in RNA levels of the six tested genes (Figure 3). EGF induced a higher magnitude of responses for all genes we analyzed. Interestingly, with both ligands we observed an oscillatory pattern of several transcripts. In conclusion, although AREG is able to initiate gene expression programs that carve biological outcomes, this requires relatively high concentrations of the growth factor.

AREG silencing in human ovarian cancer cells inhibits their tumorigenic growth in animals

To examine the prediction that AREG secretion contributes to aggressiveness of ovarian cancer, we established a model cell system using the OVCAR5 human cancer cell line that secretes relatively large quantities of AREG (see Figure 1c). Cells were transduced with viral vectors encoding either a scrambled short-hairpin RNA (shControl) or five different AREG-targeting shRNAs (shAREG). Analyses of both mRNA levels (using qPCR) and protein secretion (using ELISA) confirmed effective reduction of AREG expression by three specific hairpins (Supplementary Figure S3a). When followed in culture, the corresponding cell lines, stably expressing individual hairpins, displayed markedly reduced rates of growth (Supplementary Figure S3b). This enabled us selecting one shAREG-expressing subline of OVCAR5 cells for more detailed analyses (Figures 4a and b). Importantly, using the caspase-3 cleavage assay we found that despite retarded growth, no shAREG subline underwent detectable apoptosis (Figure 4c). Hence, in the next step, we inoculated the selected shAREG subline in the flanks of immunocompromised animals (Balb/c nude; 10 mice per group) and monitored tumor growth over a period of 4 weeks. As shown in Figure 4d, shAREG-expressing cells formed significantly smaller tumors than control cells ( $P < 0.005$ ), in agreement with their *in vitro* growth rates. Similar observations were made with OVCAR5 cells ectopically expressing other AREG-specific hairpins (Supplementary Figure S3c), and control experiments verified that the respective xenografts partly and stably lost AREG expression (Supplementary Figure S3d). In conclusion, and in line with the *in vitro* data, AREG secretion might have an important role in ovarian tumor growth, at least in an animal model system.

AREG expression is increased after treatment of ovarian cancer cells with a chemotherapeutic drug

Platinum-based antitumor agents have been the mainstay of ovarian cancer chemotherapy for the last three decades, but various mechanisms of resistance limit therapeutic efficacy.<sup>25</sup> In this context, it is interesting noting that a previous study found that resistance of MCF7 mammary cancer cells to cisplatin was accompanied by both inactivation of the p53 pathway and a selective upregulation of AREG expression.<sup>26</sup> Because the majority

of body fluids we analyzed were derived from patients treated with chemotherapy, we examined the possibility that high level secretion of AREG by ovarian and lung cancer cells is attributable to patient exposure to chemotherapeutic agents, such as cisplatin. Hence, we introduced a luciferase reporter DNA construct containing the promoter region of AREG (2297 basepairs, from SwitchGear Genomics) into both MLS ovarian cancer cells and A549 lung cancer cells. Upon treatment of cells with increasing concentrations of cisplatin, we observed 2-fold and 1.5-fold increases in the reporter activity in ovarian and in lung cells, respectively (Figures 5a and b). A similar experiment that used a luciferase reporter corresponding to TGF- $\alpha$  (or GAPDH, as a control) and MLS cells detected no consistent, cisplatin-induced changes (Supplementary Figures S4a and b). Exposure of both ovarian and lung cancer cells to the chemotherapeutic agent was followed by increased secretion of AREG, but not EGF, TGF- $\alpha$  or HB-EGF, to the medium, further supporting specificity of the cisplatin effect to the AREG promoter (Supplementary Figures S4c and d). Collectively, these results propose that the response to DNA adducts induced by platin analogs might specifically increase expression and secretion of AREG by ovarian and lung cancer cells, potentially contributing to adaptive drug resistance. Future experiments will address involvement of putative AREG's transcription factors, such as AP1 and STAT5A, in the induction by chemotherapeutic and other agents.

Generation of a mAb specific to AREG

Drugs targeting EGFR or the homologous protein ERBB2/HER2 are already used for the treatment of breast, lung, gastric, pancreatic, colorectal, and head and neck cancers.<sup>27,28</sup> Although no targeted therapy is currently available for ovarian tumors, an autocrine loop involving NRG1 and activated ERBB3 might serve as a suitable drug target.<sup>29</sup> Likewise, EGFR has been proposed,<sup>30</sup> but EGFR antagonists have so far shown only limited clinical benefits when applied on ovarian tumors.<sup>31,32</sup> Nevertheless, aberrant EGFR expression has been associated with poor outcome of ovarian cancer patients,<sup>33,34</sup> raising the possibility that targeting specific EGFR ligands might be effective. In an attempt to test this prediction, we employed a previously described approach to generate a mAb to human AREG.<sup>35</sup> First, we constructed a fusion protein comprising the EGF-like domain of AREG, a poly-histidine tag, as well as a factor Xa cleavage site. Notably, the EGF-like domain of AREG and other EGF-like ligands consists of three highly conserved disulfide bonds, which are responsible for the correct folding and activity of all ERBB ligands.<sup>36</sup> Therefore, we chose to fuse also the thioredoxin (TRX) protein to the EGF-like domain. Second, following expression in bacteria, the ligand was purified using a metal column (Figure 6a), and its ability to induce phosphorylation of EGFR was validated (Figure 6b). Next, mice were immunized with the active TRX-fused ligand and following four injections into mice, sera were obtained and examined for anti-ligand responses. Subsequently, the spleens of two mice were used to establish three hybridomas, which were screened for their ability to recognize AREG (Figure 6c). Using plasmon resonance and immunoblotting, we confirmed high-affinity binding of AR30 with human AREG (Figure 6d and Supplementary Table 3). Interestingly, AR30 did not recognize other EGFR ligands, except for weak binding to the human form of HB-EGF. Notably, it has been reported that an anti-HB-EGF antibody can bind with AREG,<sup>37</sup> suggesting that the two growth factors share structural determinants.

A monoclonal antibody to AREG inhibits ovarian tumor xenografts in animals and sensitizes them to a chemotherapeutic drug

Next, we analyzed the ability of AR30 to intercept AREG-induced phosphorylation of EGFR. As expected, AR30 reduced AREG induced EGFR phosphorylation across all concentrations of AREG we assessed (Figures 6e and f). This prompted us to investigate

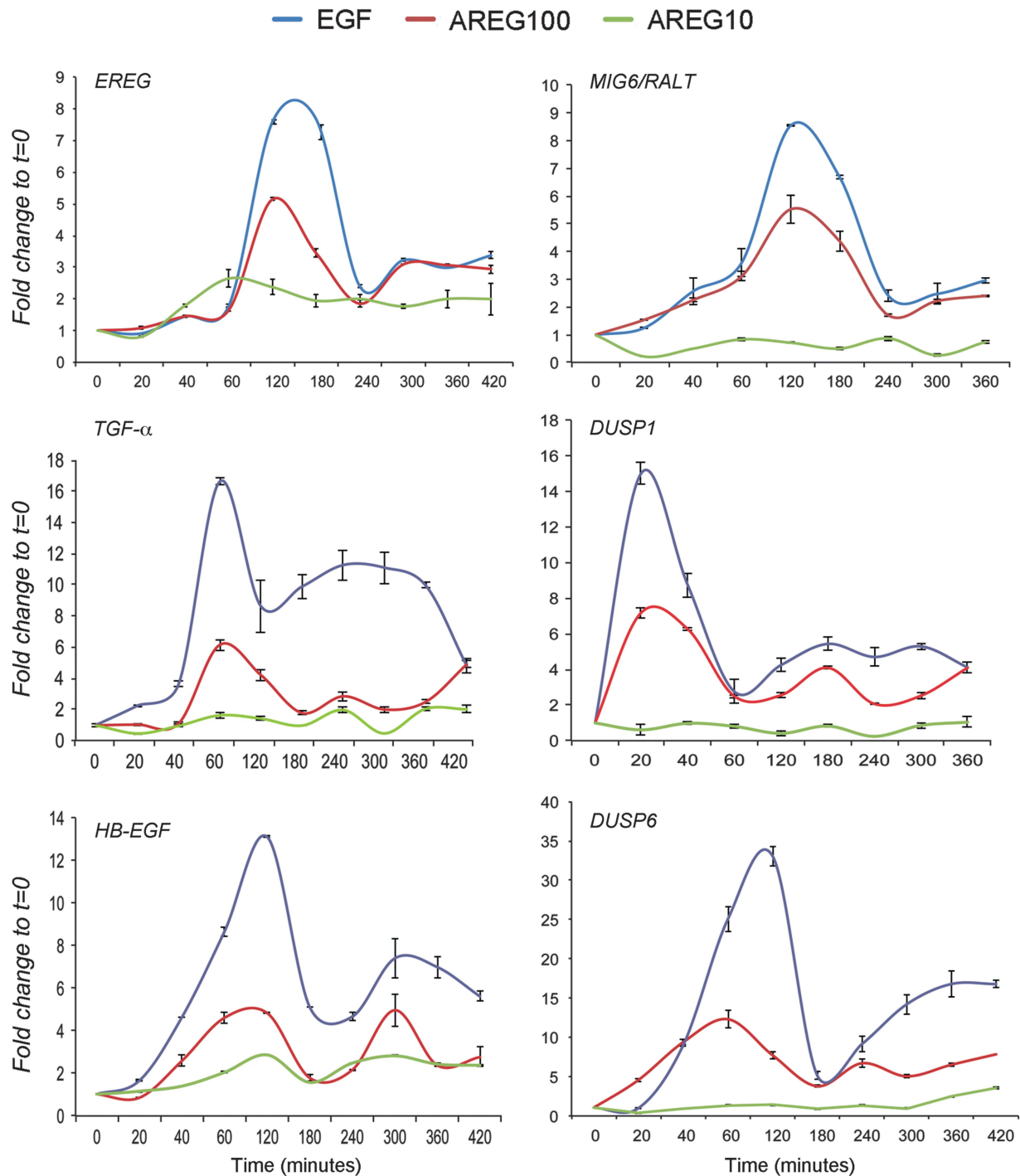


**Figure 3.** Amphiregulin acts as a weak inducer of transcription-mediated feedback regulatory loops of EGFR signaling. MCF10A cells that were starved overnight for serum factors were treated with EGF (10 ng/ml) or AREG (10 or 100 ng/ml) for the indicated time intervals. qPCR analysis was performed using primers corresponding to mRNAs encoding for either negative (*MIG6/RALT*, *DUSP1* and *DUSP6*) or positive (*EREG*, *TGF-α* and *HB-EGF*) feedback regulatory components of the EGFR signaling pathway. mRNA profiles representative of two independent biological repeats are shown.

the impact on tumorigenic growth of MLS human ovarian cancer cells, which secrete AREG but show no expression of HB-EGF (see Figure 1c). In the first set of experiments, we subcutaneously inoculated MLS cells into the flanks of female nude mice and once tumors became palpable, mice were randomized into groups of 9–11 animals. Thereafter, the antibody was injected into the peritoneum, and tumor growth was monitored over a period of 6 weeks (Figure 7a). The results showed partial inhibition of tumor

growth by AR30. Hence, our next set of animal studies tested the prediction that chemotherapy-induced upregulation of AREG secretion (see Figure 5) supports tumor growth under platinum-based treatment. Therefore, we examined a combination of cisplatin and the anti-AREG antibody. Following randomization, mice were treated with or without AR30, along with cisplatin (5 mg/kg body weight). The results presented in Figure 7b show that as single agents, both cisplatin and the AR30 antibody only

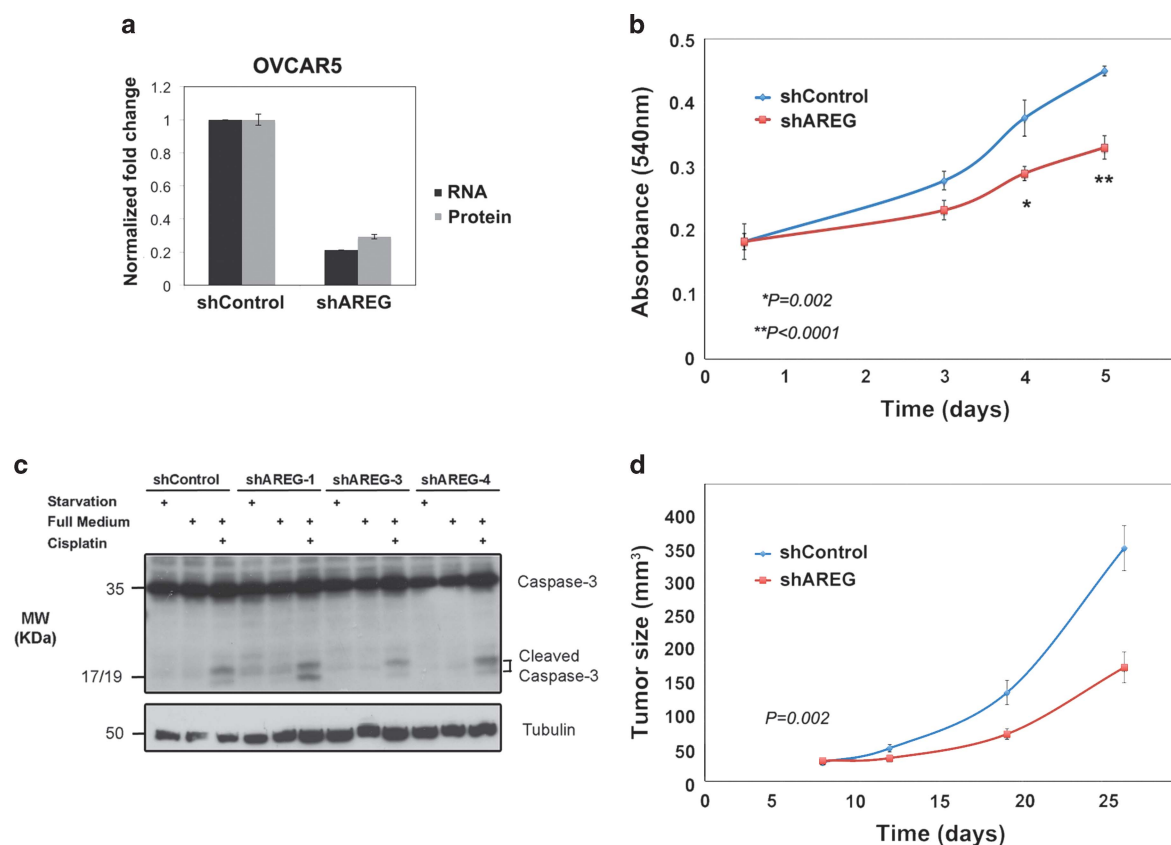


**Figure 4.** Depletion of AREG expression inhibits tumorigenic growth of human ovarian cancer cells. **(a)** OVCAR5 ovarian cancer cells were treated with lentiviral expression constructs, either a scrambled shRNA or an AREG-specific shRNA. Conditioned media were collected 3 days later and the levels of secreted AREG were assessed using ELISA. **(b)** Growth rates of shAREG or shControl OVCAR5 cells were measured using the MTT assay. Means  $\pm$  s.d. values of hexaplicates are shown. **(c)** Caspase-3 cleavage was assessed using immunoblotting and OVCAR5 sublines stably expressing three different shAREGs, or shControl. The assay was performed either in full medium or under serum starvation. Overnight treatment with cisplatin (5  $\mu$ g/ml) was used as a positive control. Note that the 35 kilodalton caspase-3 protein was cleaved only in cells incubated for 12 h in the presence of cisplatin, but no shAREG mimicked this effect. **(d)** Female nude mice (6 weeks old; 10 per group) were inoculated subcutaneously with OVCAR5 ovarian cells ( $3 \times 10^6$  per animal) pre-treated with either a scrambled shRNA or an AREG-specific shRNA. Tumor volumes were measured as indicated. Data points are presented as mean volume  $\pm$  s.d. values.

mildly inhibited MLS tumors under the conditions we selected. Nonetheless, the combination of cisplatin and AR30 almost completely inhibited tumor growth (Figures 7b and c).

In summary, using ascites and pleural fluids, we detected relatively high concentrations of AREG in the majority of advanced ovarian and lung cancer patients. Our *in vitro* studies propose that high abundance of AREG in clinical samples might reflect two processes: First, induction of AREG transcription following patient treatment with genotoxic drugs, and, second, inefficient AREG clearance by means of receptor endocytosis. Presumably, high abundance of AREG, relative to other EGF family ligands, partly compensates for the low-affinity interactions of this growth factor with EGFR. Accordingly, we show that high concentrations of AREG are needed for enhancement of tyrosine phosphorylation and induction of gene expression programs. In line with critical roles in progression of ovarian cancer, intercepting AREG using a newly generated anti-AREG antibody (denoted AR30) greatly sensitized ovarian cancer cells to a chemotherapeutic agent. These observations might open a way for clinical testing of a humanized version of AR30.

## DISCUSSION

While normal cells often send signals to neighboring cells, and the latter reciprocate by supplying various growth factors, one hallmark shared by cancer cells of various tissues of origin is their

capability to autonomously sustain proliferative signaling in a number of alternative ways.<sup>38</sup> They may overexpress a receptor for a growth factor or acquire an activating mutation in the receptor, or in downstream signaling pathways. Alternatively, they may produce growth factor ligands, to which they can respond via the expression of cognate receptors, resulting in autocrine proliferative stimulation.<sup>39</sup> EGFR well exemplifies this attribute of transformed cells: on the one hand, ductal morphogenesis of the mammary gland is regulated by a paracrine mechanism that involves shedding of AREG by epithelial cells and subsequent stimulation of EGFR of stromal cells.<sup>14</sup> On the other hand, co-expression of EGFR and AREG characterizes a wide variety of carcinomas and skin tumors (reviewed by Berasain and Avila<sup>11</sup>). This extends to several other ligands, which are co-expressed with EGFR in a variety of tumors.<sup>40</sup>

For the last decade, intercepting EGFR signaling using kinase inhibitors or mAbs has become a mainstay clinical protocol, for example in the treatment of lung and colorectal cancers, respectively. However, rather weak responses that are limited to small groups of patients, along with early onset of resistance to drugs, currently limit clinical applications. Nevertheless, several newer strategies are under development, including specific aptamers<sup>41</sup> and combinations of 2–3 antibodies, each directed at a distinct receptor's epitope.<sup>42,43</sup> Directly intercepting EGFR's ligands represents another potential approach to improve

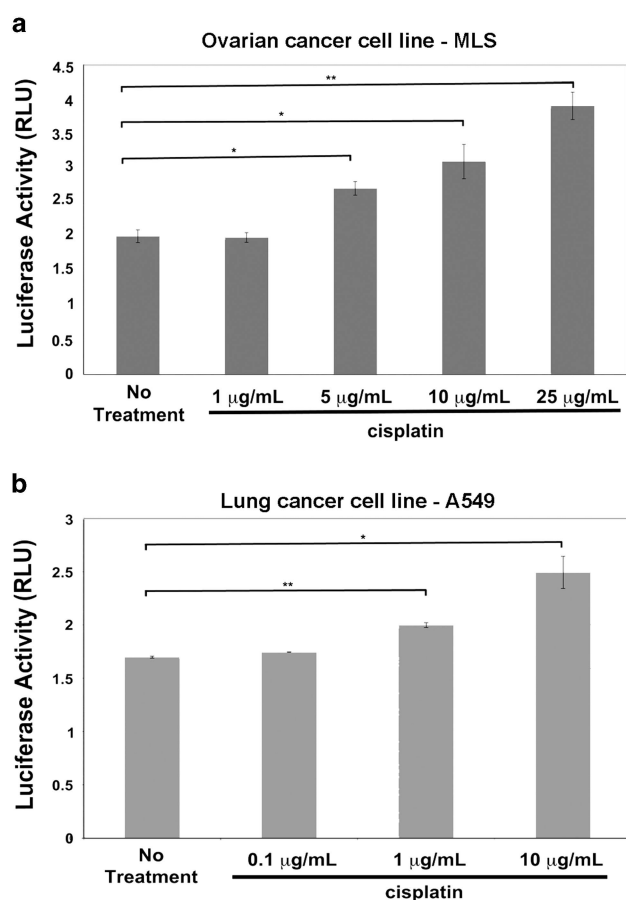


**Figure 5.** Transcriptional activation of the AREG promoter by cisplatin. **(a)** MLS cells were transfected with a luciferase reporter containing the promoter region of AREG. Luciferase activity derived from the *Renilla* luciferase was determined and normalized to that derived from the firefly luciferase reporter. Twenty-four hours after transfection, increasing concentrations of cisplatin were added and 48 h later the cells were subjected to luciferase assays. **(b)** A549 lung cancer cells were treated as in **(a)**. Averages of triplicates and s.d. values (bars) are presented (\* $P < 0.03$ , \*\* $P < 0.01$ ,  $t$ -test).

response benefit. A decoy recombinant fusion protein containing portions of EGFR and ERBB4/HER4 was able to inhibit all ligands of the EGF family, as well as retard growth of several tumor xenografts.<sup>44</sup> To reduce toxicity, it might be critical to intercept fewer ligands, within the context of specific tumors. For example, we previously demonstrated that co-inhibition of TGF- $\alpha$  and HB-EGF, using a mixture of the respective mAbs, effectively retarded tumorigenic growth of several xenografts.<sup>35</sup> Knowing the repertoire of growth factors produced by a given primary or secondary tumor, as well as by cells in the microenvironment, is a prerequisite, here we offer liquid biopsies as one way to sample both microenvironments and the tumors they nest, even those tumors that may not be easily imaged or localized.

Ascites and pleural fluids of cancer patients are routinely available, often in quite large volumes. The common denominator of the majority of the 61 fluids we analyzed (from ovarian and lung cancer patients) has been high concentrations and almost ubiquitous presence of AREG (Figure 1). High AREG expression has already been validated as a marker of better response of colorectal cancer patients to EGFR-targeting mAbs.<sup>45</sup> Similarly, in lung cancer patients treated with gefitinib or erlotinib, high AREG was associated with stable, rather than progressive disease.<sup>46</sup> Thus, AREG might serve as a predictor of patient response, and probably also as a target for combination therapy, as we elaborate herein.

The logic behind the common occurrence and high abundance of AREG in liquid biopsies might be attributed to several aspects of the biology of AREG: clearance of AREG from the circulation might be retarded by binding to heparin sulfate proteoglycans, as well as by the relatively low EGFR binding affinity of this ligand,<sup>15</sup> along with its tendency to increase receptor recycling rather than receptor degradation (see Figure 2).<sup>19–21</sup> The effect of slow clearance might be augmented by more rapid rates of AREG synthesis, especially in patients undergoing treatment with cytotoxic drugs, or in patients displaying high estrogen concentrations.<sup>47</sup> In addition, several attributes associated with advanced tumors have been linked to AREG induction. The list includes chronic inflammation,<sup>48</sup> high serum levels of the lysophosphatidic acid<sup>49</sup> and expression of a mutant form of p53.<sup>50</sup>

The biological and clinical features of AREG, along with frequent expression in ascites fluids obtained from chemotherapy-treated, advanced ovarian cancer patients, prompted us to generate a new antibody to the human factor, and test it on xenografts of human ovarian cancer. It is worth mentioning that only 20% of ovarian cancers are diagnosed while they are limited to the ovaries, and although at least 70% of patients will initially respond to a combination of platinum- and taxane-based therapy, the majority will develop resistance and eventually progress (reviewed in Bast *et al.*<sup>51</sup>). Importantly, when singly applied on ovarian xenografts the antibody we generated, denoted AR30, induced only moderate effects on tumor growth. While the partial anti-tumor effect of AR30 might be due to an inability to completely block AREG-induced auto-phosphorylation of EGFR, the combination with cisplatin remarkably inhibited growth of ovarian tumors in animals. This observation raises the possibility that anti-AREG antibodies may greatly increase the activity of platin analogs in patients, either as an upfront therapy or for patients who are initially platin sensitive but become platin resistant. While this prediction is a matter for future investigation, it is worthwhile noting that AREG expression has been correlated with resistance to chemotherapeutic agents,<sup>26</sup> as well as with resistance of hepatocellular carcinoma to sorafenib, a multi-target kinase inhibitor.<sup>52</sup> Whether or not AR30 and derivative humanized molecules will act upon AREG-expressing, therapy-resistant tumors of ovarian, liver and other origins remains an open question.

## MATERIALS AND METHODS

### Materials and cell lines

The following antibodies were used: anti-EGFR from Enzo Life Science (Farmingdale, NY, USA), anti-phospho EGFR (pTyr1068), anti-caspase-3 (clone 8G10), anti-phospho-ERK1/ERK2 (Thr202/Tyr204—clone D13.14.4E) from Cell Signaling Technology (Danvers, MA, USA), anti-phospho tyrosine (PY99), ERK2, anti-ubiquitin (clone P4D1) from Santa Cruz Biotechnology (Santa Cruz, CA, USA) and anti-tubulin from Sigma-Aldrich (St Louis, MO, USA). All growth factors were from Peprotech (Rocky Hill, NJ, USA). Cells were purchased from the American Type Culture Collection (ATCC). Both ovarian and lung cell lines were grown in RPMI-1640 supplemented with 10% fetal calf serum and 1% PenStrep (100 U/ml Penicillin and 100  $\mu\text{g/mL}$  Streptomycin), with the exception of OVCAR3 cells, which were grown in 20% fetal calf serum. The levels of the EGF-family ligands AREG, BTC, EGF, HB-EGF, NRG1 and TGF- $\alpha$  were analyzed using an ELISA kit (DuoSet ELISA kit—R&D Systems, Minneapolis, MN, USA).

### Patient specimens

Ascites fluids from ovarian cancer patients and pleural effusions from lung cancer patients were collected at the Sheba Medical Center in Tel Hashomer (Israel) following consent, as part of the Institutional Tissue Banks (IRB approvals #2090-00, #5684-08 and #0775-13). The presented study was approved by the Ethics Committee of the Sheba Medical Center (IRB approval #7891-09).



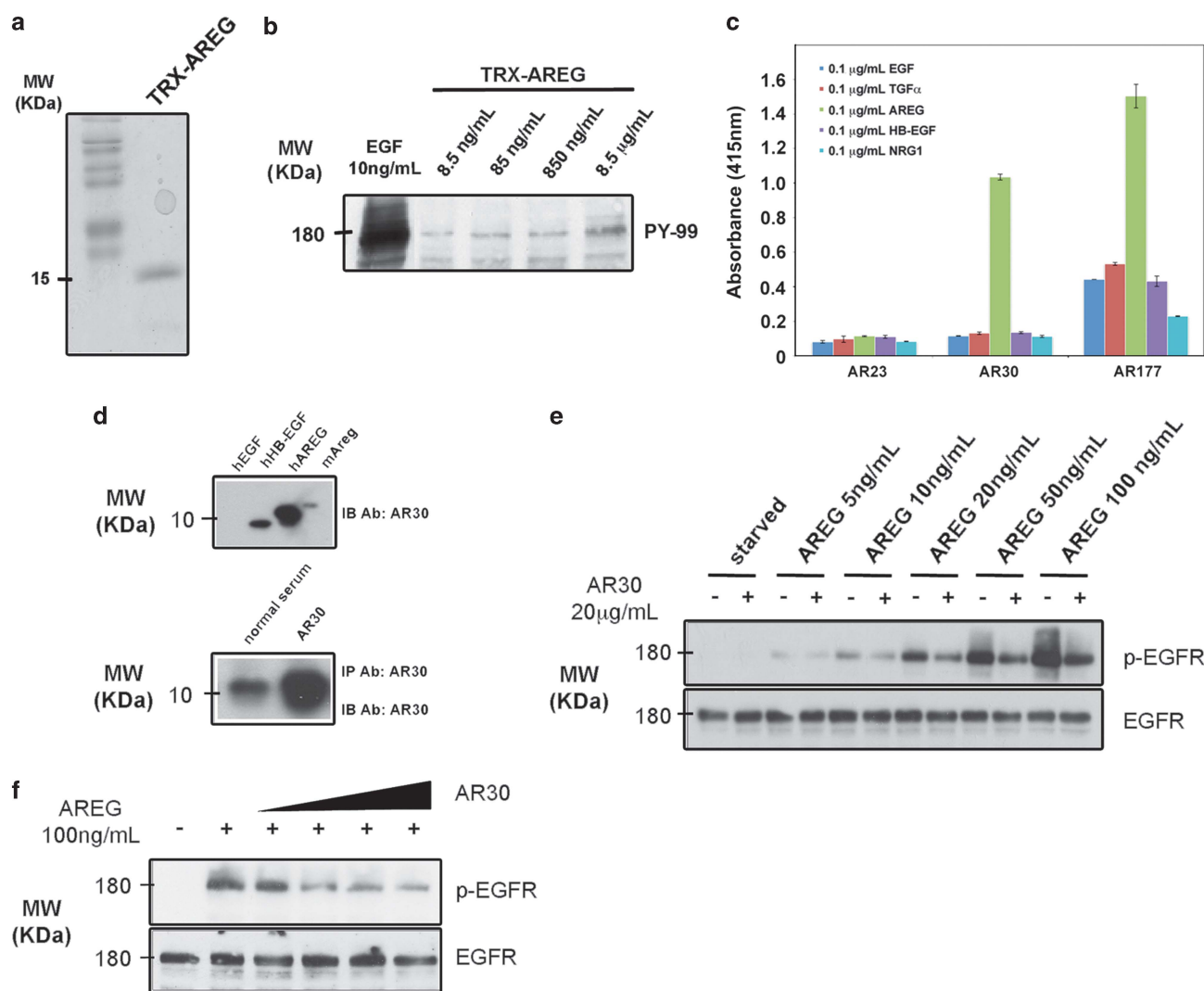


**Figure 6.** AR30, an anti-AREG monoclonal antibody, inhibits auto-phosphorylation of EGFR. **(a)** Coomassie blue staining of an acrylamide gel showing a purified fraction of AREG isolated from bacteria and purified on a NiNTA column. The molecular weight marker lane indicates a 15-kilodalton band. **(b)** Cells were seeded in a 24-well plate, washed and incubated with increasing concentrations of the purified TRX-AREG fusion protein (8.5, 85, 850 and 8500 ng/ml). EGF (10 ng/ml) was used as a positive control. Following a 10-min long incubation, the cells were lysed and cleared extracts immunoblotted (IB) with an anti-phosphotyrosine antibody (PY-99). **(c)** 96-well plates were coated with the indicated ligands (0.1 µg/ml), and then incubated for 3 h with three different mAbs specific to AREG. Thereafter, wells were incubated for 2 h with an anti-mouse antibody conjugated to HRP, followed by a 30-min incubation with ATBS. Signals were determined using an ELISA reader (set at 415 nm). **(d)** Human EGF, HB-EGF and AREG, as well as murine AREG, were immunoblotted (IB) with the AR30 mAb, either directly (upper panel) or following immunoprecipitation (IP) using the same antibody (lower panel). Serum from non-immunized mice was used as a negative control. **(e)** HeLa cells were pre-incubated with (or without) mAb AR30 (20 µg/ml) and increasing concentrations of AREG. Thereafter, whole-cell lysates were immunoblotted (IB) using an antibody specific to the phosphorylated form of EGFR (tyrosine 1068) or an antibody to EGFR. **(f)** HeLa cells were incubated with (or without) AREG (100 ng/ml) in the presence of increasing concentrations of mAb AR30 (5, 10, 20 and 50 µg/ml). Thereafter, cells were lysed and cleared extracts immunoblotted (IB) using the indicated antibodies.

#### Ligand displacement, receptor ubiquitination and downregulation assays

Previously described protocols were used.<sup>5</sup>

#### RNA isolation and qPCR

Total RNA was extracted using the PerfectPure RNA Cultured Cell Kit (5-prime, Hamburg, Germany) according to the manufacturer's instructions. Total RNA quantity and quality were determined using the NanoDrop ND-1000 Spectrophotometer (Thermo Fischer Scientific, Waltham, MA, USA). Complementary DNA was synthesized using the High Capacity Reverse Transcription kit (Applied Biosystems, Life Technologies, Carlsbad, CA, USA). The nucleotide sequences of primers for the positive regulators (*EREG*, *TGF-α* and *HB-EGF*), negative regulators (*MIG6/RALT*, *DUSP1* and *DUSP6*) and beta2-microglobulin (*B2M*) are shown in Supplementary Table 4.

The KiCqStart primers from Sigma-Aldrich were used to detect the levels of human *AREG* (H\_AREG\_3). Real-time qPCR analysis was performed with SYBR Green (Applied Biosystems) and specific primers on the StepOne Plus Real-Time PCR system (Applied Biosystems). qPCR signals (Ct) were normalized to *B2M*.

#### Lentiviral constructs

shRNAs targeting AREG were obtained from Sigma-Aldrich. The vector for the scrambled shRNA was obtained from Addgene (Cambridge, MA, USA; plasmid 1864). Lentiviruses were packaged by co-transfection of constructs with the Sigma-Aldrich MISSION Lentiviral Packaging Mix. In brief, lentiviruses were produced by transfection of HEK293FT cells with Lipofectamine 2000 (Invitrogen, Life Technologies) according to the manufacturer's protocol. OVCAR5 cells were subsequently infected and selected with 2 µg/ml of puromycin to create the stable shControl and



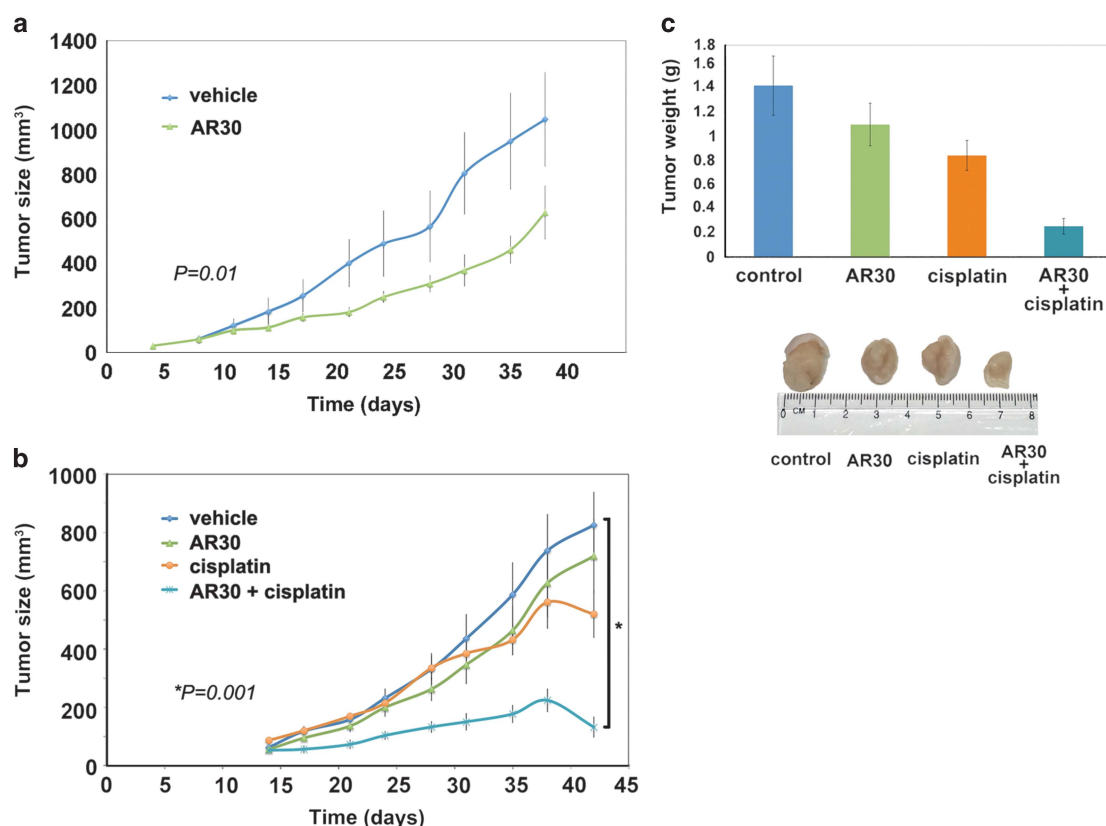


**Figure 7.** An anti-AREG monoclonal antibody inhibits tumorigenic growth of human ovarian cancer cells in mice. **(a)** Female nude mice (6 weeks old) were inoculated subcutaneously with MLS ovarian cancer cells ( $2 \times 10^6$  per animal). Once tumors became palpable, mice were randomized into two groups. Eleven mice were injected intraperitoneally with an anti-AREG mAb (AR30; 200  $\mu$ g/mouse; twice a week, on days: 8, 11, 14, 17 and 21). The control group also included 11 mice. Means  $\pm$  s.d. values are shown. **(b)** Female nude mice (6 weeks old) were inoculated subcutaneously with MLS ovarian cancer cells ( $2 \times 10^6$  per animal). Once tumors became palpable, mice were randomized into four groups. One group (8 mice) was injected intraperitoneally with the AR30 mAb (100  $\mu$ g/mouse twice a week, on days: 8, 14, 17, 21, 24 and 28). Another group (8 mice) was treated with cisplatin (5 mg/kg; on days 8 and 21). The fourth group was treated with a combination of mAb AR30 and cisplatin. The control group included 12 mice. **(c)** The indicated MLS tumors were excised, and their average weights determined. Representative tumors were photographed.

shAREG cell lines. The efficacy of AREG knockdown was assessed at the RNA level using qPCR, and at the protein level by means of ELISA.

#### Luciferase reporter assays

For promoter reporter assays, MLS and A549 cells were co-transfected with a commercially available Renilla luciferase plasmid containing the promoter region of *AREG*, *TGF- $\alpha$* , a positive control of promoter activity, namely *GAPDH*, or a random control vector *R01*, which we used as a negative control (SwitchGear Genomics, Menlo Park, CA, USA). Additionally, the pGL3-Control vector containing Firefly luciferase (Promega, Madison, WI, USA) was transfected as a control for transfection efficiency. Promoter activity was determined using the dual-luciferase reporter assay system according to the manufacturer's instructions (Promega). Renilla luciferase luminescence values were normalized to Firefly luminescence and quantified relative to control.

#### Surface plasmon resonance measurements

Surface plasmon resonance was performed on a BIAcore 3000 instrument (BIAcore, Uppsala, Sweden). Proteins were diluted in 100 mM Na-acetate (pH 4.6) to 20  $\mu$ g/ml and immobilized on a CM5 sensor chip. The protein solution was flown over the chip for 5 min at a rate of 20  $\mu$ l/min. The binding assay was performed by injecting the analyte solutions at 25  $^{\circ}$ C at eight different concentrations (depending on the ligand: hAREG 1–30 nM, mAREG 500–5000 nM, hHB-EGF 1–100 nM and mHB-EGF 1–20  $\mu$ M). These conditions resulted in a linear relation between protein concentration and maximal (steady-state) response, indicating a pseudo first-order regime in relation to the immobilized ligand. The association phase of analyte binding to all ligands was followed for 4 min, and dissociation phases were monitored for

3 min. The response was monitored as a function of time (sensorgram). Multi-concentration data underwent fitting using the software BIAevaluation 3.2 (BIAcore/GE Healthcare, Little Chalfont, UK).

#### Xenograft mouse models

All animal procedures were approved by the Weizmann Institute of Science's review board. Female athymic NCr-nude mice (6 weeks old) were inoculated subcutaneously with  $2 \times 10^6$  human ovarian MLS cancer cells. Once tumors became palpable (5–7 days), the mice were randomized into groups and injected intraperitoneally at the indicated time points with a mAb, chemotherapy or the combination. Tumor volumes were monitored twice a week, and body weights were measured once a week.

#### CONFLICT OF INTEREST

The authors declare no conflict of interest.

#### ACKNOWLEDGEMENTS

We thank Julian Downward for lung cell lines. This work was performed at the Marvin Tanner Laboratory for Cancer Research and it was supported, in part, by Merck KGaA. The research in our laboratory is supported by the Israel Cancer Research Fund and the Dr Miriam and Sheldon G Adelson Medical Research Foundation and by the MD Moross Institute for Cancer Research. YY is the incumbent of the Harold and Zelda Goldenberg Professorial Chair. The Sheba Institutional Tissue Banks have received financial support from the Flight Attendants Medical Research Institute (FAMRI).

## REFERENCES

- Witsch E, Sela M, Yarden Y. Roles for growth factors in cancer progression. *Physiology (Bethesda)* 2010; **25**: 85–101.
- Burgess AW. EGFR family: structure physiology signalling and therapeutic targets. *Growth Factors* 2008; **26**: 263–274.
- Hynes NE, MacDonald G. ErbB receptors and signaling pathways in cancer. *Curr Opin Cell Biol* 2009; **21**: 177–184.
- Wilson JT, Akita RW, Sliwkowski MX. Binding specificities and affinities of egf domains for ErbB receptors. *FEBS Lett* 1999; **447**: 227–231.
- Kochupurakkal BS, Harari D, Di-Segni A, Maik-Rachline G, Lyass L, Gur G et al. Epigen, the last ligand of ErbB receptors, reveals intricate relationships between affinity and mitogenicity. *J Biol Chem* 2005; **280**: 8503–8512.
- Amit I, Citri A, Shay T, Lu Y, Katz M, Zhang F et al. A module of negative feedback regulators defines growth factor signaling. *Nat Genet* 2007; **39**: 503–512.
- Lazzara MJ, Lauffenburger DA. Quantitative modeling perspectives on the ErbB system of cell regulatory processes. *Exp Cell Res* 2009; **315**: 717–725.
- Reddy CC, Niyogi SK, Wells A, Wiley HS, Lauffenburger DA. Engineering epidermal growth factor for enhanced mitogenic potency. *Nat Biotechnol* 1996; **14**: 1696–1699.
- Tzahar E, Moyer JD, Waterman H, Barbacci EG, Bao J, Levkowitz G et al. Pathogenic poxviruses reveal viral strategies to exploit the ErbB signaling network. *EMBO J* 1998; **17**: 5948–5963.
- Wilson KJ, Mill C, Lambert S, Buchman J, Wilson TR, Hernandez-Gordillo V et al. EGFR ligands exhibit functional differences in models of paracrine and autocrine signaling. *Growth factors (Chur, Switzerland)* 2012; **30**: 107–116.
- Berasain C, Avila MA. Amphiregulin. *Semin Cell Dev Biol* 2014; **28C**: 31–41.
- Willmarth NE, Ethier SP. Autocrine and juxtacrine effects of amphiregulin on the proliferative, invasive, and migratory properties of normal and neoplastic human mammary epithelial cells. *J Biol Chem* 2006; **281**: 37728–37737.
- Higginbotham JN, Demory Beckler M, Gephart JD, Franklin JL, Bogatcheva G, Kremers GJ et al. Amphiregulin exosomes increase cancer cell invasion. *Curr Biol* 2011; **21**: 779–786.
- Sternlicht MD, Sunnarborg SW, Kourois-Mehr H, Yu Y, Lee DC, Werb Z. Mammary ductal morphogenesis requires paracrine activation of stromal EGFR via ADAM17-dependent shedding of epithelial amphiregulin. *Development* 2005; **132**: 3923–3933.
- Shoyab M, Plowman GD, McDonald VL, Bradley JG, Todaro GJ. Structure and function of human amphiregulin: a member of the epidermal growth factor family. *Science* 1989; **243**: 1074–1076.
- DeWitt A, Iida T, Lam HY, Hill V, Wiley HS, Lauffenburger DA. Affinity regulates spatial range of EGF receptor autocrine ligand binding. *Dev Biol* 2002; **250**: 305–316.
- Ebner R, Derynck R. Epidermal growth factor and transforming growth factor- $\alpha$ : differential intracellular routing and processing of ligand-receptor complexes. *Cell Regul* 1991; **2**: 599–612.
- Levkowitz G, Waterman H, Zamir E, Kam Z, Oved S, Langdon WY et al. c-Cbl/Sli-1 regulates endocytic sorting and ubiquitination of the epidermal growth factor receptor. *Genes Dev* 1998; **12**: 3663–3674.
- Stern KA, Place TL, Lill NL. EGF and amphiregulin differentially regulate Cbl recruitment to endosomes and EGF receptor fate. *Biochem J* 2008; **410**: 585–594.
- Baldys A, Gooz M, Morinelli TA, Lee MH, Raymond JR Jr, Luttrell LM et al. Essential role of c-Cbl in amphiregulin-induced recycling and signaling of the endogenous epidermal growth factor receptor. *Biochemistry* 2009; **48**: 1462–1473.
- Roepstorff K, Grandal MV, Henriksen L, Knudsen SL, Lerdrup M, Grovdal L et al. Differential effects of EGFR ligands on endocytic sorting of the receptor. *Traffic* 2009; **10**: 1115–1127.
- Zhang Y, Yarden Y. Systems biology of growth factor-induced receptor endocytosis. *Traffic* 2009; **10**: 349–363.
- Frosi Y, Anastasi S, Ballaro C, Varsano G, Castellani L, Maspero E et al. A two-tiered mechanism of EGFR inhibition by RALT/MIG6 via kinase suppression and receptor degradation. *J Cell Biol* 2010; **189**: 557–571.
- Keyse SM. Dual-specificity MAP kinase phosphatases (MKPs) and cancer. *Cancer Metastasis Rev* 2008; **27**: 253–261.
- Lopez J, Banerjee S, Kaye SB. New developments in the treatment of ovarian cancer—future perspectives. *Ann Oncol* 2013; **24**: x69–x76.
- Eckstein N, Servan K, Girard L, Cai D, von Jonquieres G, Jaehde U et al. Epidermal growth factor receptor pathway analysis identifies amphiregulin as a key factor for cisplatin resistance of human breast cancer cells. *J Biol Chem* 2008; **283**: 739–750.
- Arteaga CL, Sliwkowski MX, Osborne CK, Perez EA, Puglisi F, Gianni L. Treatment of HER2-positive breast cancer: current status and future perspectives. *Nat Rev Clin Oncol* 2012; **9**: 16–32.
- Yarden Y, Pines G. The ERBB network: at last, cancer therapy meets systems biology. *Nat Rev Cancer* 2012; **12**: 553–563.
- Sheng Q, Liu X, Fleming E, Yuan K, Piao H, Chen J et al. An activated ErbB3/NGR1 autocrine loop supports in vivo proliferation in ovarian cancer cells. *Cancer Cell* 2010; **17**: 298–310.
- Gui T, Shen K. The epidermal growth factor receptor as a therapeutic target in epithelial ovarian cancer. *Cancer Epidemiol* 2012; **36**: 490–496.
- Siwak DR, Carey M, Hennessy BT, Nguyen CT, McGahren Murray MJ, Nolden L et al. Targeting the epidermal growth factor receptor in epithelial ovarian cancer: current knowledge and future challenges. *J Oncol* 2010; **2010**: 568938.
- Murphy M, Stordal B. Erlotinib or gefitinib for the treatment of relapsed platinum pretreated non-small cell lung cancer and ovarian cancer: a systematic review. *Drug Resist Updat* 2011; **14**: 177–190.
- Lassus H, Sihto H, Leminen A, Joensuu H, Isola J, Nupponen NN et al. Gene amplification, mutation, and protein expression of EGFR and mutations of ERBB2 in serous ovarian carcinoma. *J Mol Med (Berl)* 2006; **84**: 671–681.
- Brustmann H. Epidermal growth factor receptor expression in serous ovarian carcinoma: an immunohistochemical study with galectin-3 and cyclin D1 and outcome. *Int J Gynecol Pathol* 2008; **27**: 380–389.
- Lindzen M, Lavi S, Leitner O, Yarden Y. Tailored cancer immunotherapy using combinations of chemotherapy and a mixture of antibodies against EGF-receptor ligands. *Proc Natl Acad Sci USA* 2010; **107**: 12559–12563.
- Van Zoelen EJ, Stortelers C, Lenferink AE, Van de Poll ML. The EGF domain: requirements for binding to receptors of the ErbB family. *Vitam Horm* 2000; **59**: 99–131.
- Sato S, Drake AW, Tsuji I, Fan J. A potent anti-HB-EGF monoclonal antibody inhibits cancer cell proliferation and multiple angiogenic activities of HB-EGF. *PLoS ONE* 2012; **7**: e51964.
- Hanahan D, Weinberg RA. Hallmarks of cancer: the next generation. *Cell* 2011; **144**: 646–674.
- Sporn MB, Todaro GJ. Autocrine secretion and malignant transformation of cells. *N Engl J Med* 1980; **303**: 878–880.
- Normanno N, Bianco C, Strizzi L, Mancino M, Maiello MR, De Luca A et al. The ErbB receptors and their ligands in cancer: an overview. *Curr Drug Targets* 2005; **6**: 243–257.
- Esposito CL, Passaro D, Longobardo I, Condorelli G, Marotta P, Affuso A et al. A neutralizing RNA aptamer against EGFR causes selective apoptotic cell death. *PLoS ONE* 2011; **6**: e24071.
- Pedersen MW, Jacobsen HJ, Koefoed K, Hey A, Pyke C, Haurum JS et al. Sym004: a novel synergistic anti-epidermal growth factor receptor antibody mixture with superior anticancer efficacy. *Cancer Res* 2010; **70**: 588–597.
- Friedman LM, Rinon A, Schechter B, Lyass L, Lavi S, Bacus SS et al. Synergistic down-regulation of receptor tyrosine kinases by combinations of mAbs: implications for cancer immunotherapy. *Proc Natl Acad Sci USA* 2005; **102**: 1915–1920.
- Lindzen M, Carvalho S, Starr A, Ben-Chetrit N, Pradeep CR, Kostler WJ et al. A recombinant decoy comprising EGFR and ErbB-4 inhibits tumor growth and metastasis. *Oncogene* 2012; **31**: 3505–3515.
- Khambata-Ford S, Garrett CR, Meropol NJ, Basik M, Harbison CT, Wu S et al. Expression of epiregulin and amphiregulin and K-ras mutation status predict disease control in metastatic colorectal cancer patients treated with cetuximab. *J Clin Oncol* 2007; **25**: 3230–3237.
- Yonesaka K, Zejnullahu K, Lindeman N, Homes AJ, Jackman DM, Zhao F et al. Autocrine production of amphiregulin predicts sensitivity to both gefitinib and cetuximab in EGFR wild-type cancers. *Clin Cancer Res* 2008; **14**: 6963–6973.
- Ciarloni L, Mallepell S, Briskin C. Amphiregulin is an essential mediator of estrogen receptor  $\alpha$  function in mammary gland development. *Proc Natl Acad Sci USA* 2007; **104**: 5455–5460.
- Hsu D, Fukata M, Hernandez YG, Sotolongo JP, Goo T, Maki J et al. Toll-like receptor 4 differentially regulates epidermal growth factor-related growth factors in response to intestinal mucosal injury. *Lab Invest* 2010; **90**: 1295–1305.
- Panupinthu N, Yu S, Zhang D, Zhang F, Gagea M, Lu Y et al. Self-reinforcing loop of amphiregulin and Y-box binding protein-1 contributes to poor outcomes in ovarian cancer. *Oncogene* 2013; **33**: 2846–2856.
- Sauer L, Gitenay D, Vo C, Baron VT. Mutant p53 initiates a feedback loop that involves Egr-1/EGF receptor/ERK in prostate cancer cells. *Oncogene* 2010; **29**: 2628–2637.
- Bast RC Jr., Hennessy B, Mills GB. The biology of ovarian cancer: new opportunities for translation. *Nat Rev Cancer* 2009; **9**: 415–428.
- Blivet-Van Eggelpeel M-J, Chettouh H, Fartoux L, Aoudjehane L, Barbu V, Rey C et al. Epidermal growth factor receptor and HER-3 restrict cell response to sorafenib in hepatocellular carcinoma cells. *J Hepatol* 2012; **57**: 108–115.

Supplementary Information accompanies this paper on the Oncogene website (<http://www.nature.com/onc>)